

## UV laser radiation for microstructuring of photostructurable glasses

Ulrike Brokmann, Alf Harnisch, Werner Ertel-Ingrisch and Dagmar Hülsenberg  
Technische Universität Ilmenau, Ilmenau (Germany)

Photostructurable glasses are important materials for applications in microsystems. They enable structures with high aspect ratios and a high dependability of mechanical, optical and chemical properties in a large range of temperatures. The exposure of photostructurable glasses to UV laser radiation, as a rapid prototyping technique, is an alternative method to the exposure by a mask aligner.

A photostructurable glass (FS21) was exposed to UV laser radiation of the wavelengths 248, 308 and 355 nm. Investigated was the influence of the exposure parameters wavelength of laser radiation and energy density on structuring results such as crystallization depth, lateral geometry of crystallized areas, structure of crystallized areas and etch angle for single pulse exposure.

### 1. Introduction

Glasses are important materials for engineering of microsystems in many fields. Main reasons are the transparency of the material in a large range of wavelength, high thermal strength and extremely high mechanical strength of miniaturized glass structures. Some applications are mechanical elements like micromechanical grippers and springs, components for microfluidic or microreaction technique and micro-optical elements [1 and 2]. The structuring technologies are multifaceted and their exertion depends on definite requirements.

The structuring process is divided into three steps, as shown in figure 1. A photochemical modification of the exposed areas takes place during the first step [3]. Due to the UV exposure of the glass,  $Ce^{3+}$  ions will be stimulated to donate one photoelectron for reduction of  $Ag^+$  ions. In a second step, during the thermal treatment, in these exposed areas, silver atoms agglomerate to clusters and build a nucleus for the crystallization of lithium metasilicate. The microstructuring of the glass in the proper meaning of the word takes place in the third step, the wet chemical etching in diluted hydrofluoric acid.

Different technologies of exposure of photostructurable glasses are possible. State of the art is the exposure as a batch process by using a mask aligner. Due to the transparency in the UV range, a mask of fused silica with a structured chromium layer is necessary. For manufacturing prototypes, this has some drawbacks regarding the high

costs of such masks. Exposure techniques that use UV laser radiation are more flexible. For instance writing techniques and dynamic mask projection are possible. Therefore, the UV laser exposure of photostructurable glasses belongs to the so-called rapid prototyping techniques (figure 1).

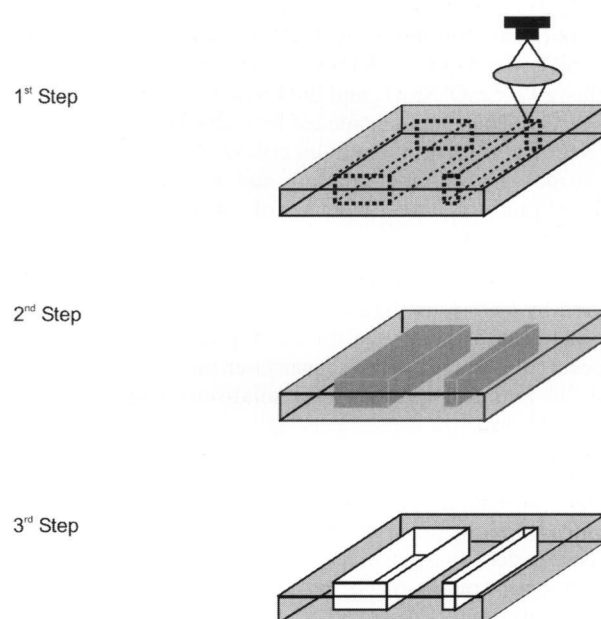


Figure 1. Microstructuring process of photostructurable glass with UV laser exposure; 1<sup>st</sup> step: UV laser exposure, 2<sup>nd</sup> step: thermal treatment, 3<sup>rd</sup> step: wet chemical etching.

Received 24 November 2003.

Presented in German at 77<sup>th</sup> Annual Meeting of the German Society of Glass Technology in Leipzig (Germany) on 28 May 2003.

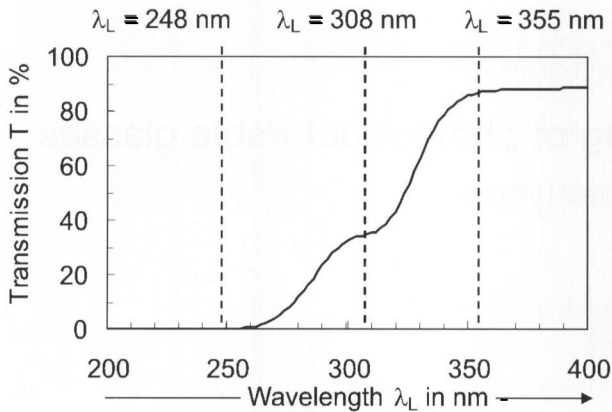


Figure 2. Spectral transmission of the glass FS21 in the UV range. In addition the wavelengths of the later used laser radiations are marked.

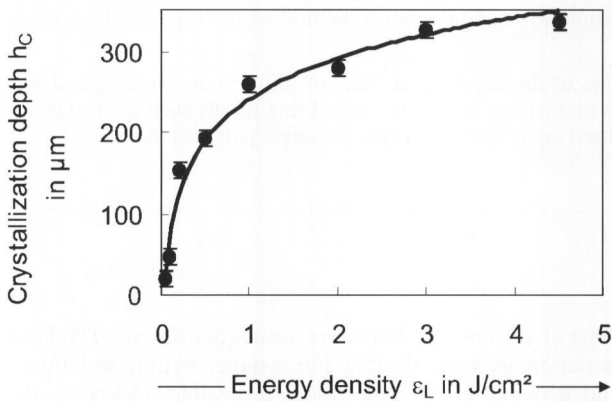


Figure 3. Crystallization depth  $h_C$  after single pulse exposure with  $\lambda_L = 248$  nm and thermal treatment dependent on energy density  $\epsilon_L$ .

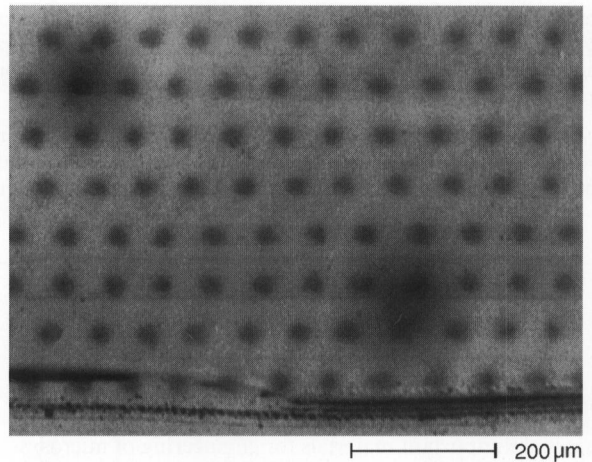
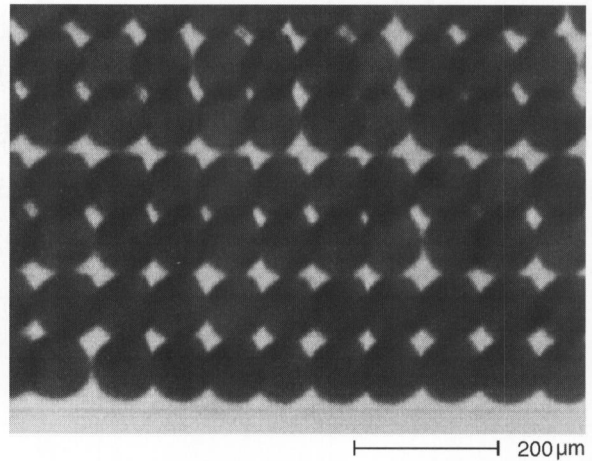
## 2. Experimental

The photostructurable glass FS21 (composition in mol%) 69.3 SiO<sub>2</sub>, 4.0 Al<sub>2</sub>O<sub>3</sub>, 21.8 LiO<sub>2</sub>, 2.5 Na<sub>2</sub>O, 2.5 K<sub>2</sub>O is doped with Ag<sub>2</sub>O, Ce<sub>2</sub>O, Sb<sub>2</sub>O<sub>3</sub> and SnO to achieve photosensitive properties. This glass was melted by a laboratory method in an electrical furnace in platinum crucibles. After the process steps molding, cutting, grinding and polishing, the semi-finished products have a diameter of 7.4 cm and a thickness of about 700 μm.

FS21 glass has an absorption band at  $\lambda = 310$  nm, caused by Ce<sup>3+</sup> ions (figure 2). In figure 2 are also marked the wavelengths later used for the UV laser exposure. The exposure took place with excimer laser radiation ( $\lambda_L = 248$  and 308 nm) and (3 $\omega$ )Nd:YAG solid-state laser radiation ( $\lambda_L = 355$  nm).

Following laser parameters are important in order to obtain the desired structures:

- wavelength of the laser radiation  $\lambda_L$  in nm,
- energy density  $\epsilon_L$  in J/cm<sup>2</sup>,
- number of pulses  $N$ ,
- pulse duration  $\tau$  in ns,
- diameter of the laser beam at the imaging surface  $d_L$  in μm,
- focal position regarding the exposure topside,
- local beam profile.



Figures 4a and b. Crystallized structures after single pulse laser exposure  $\epsilon_L = 1$  J/cm<sup>2</sup>, with a)  $\lambda_L = 248$  nm,  $d_L = 92$  μm and thermal treatment, and b)  $\lambda_L = 355$  nm,  $d_L = 80$  μm and thermal treatment.

The thermal treatment took place at 590 °C for 1 h. Exposed glass samples were positioned on a coated stainless steel plate in an electrical furnace. After this process, the exposed areas were partially crystallized to lithium metasilicate and were brown colored.

The crystallized areas were analyzed under a light optical microscope to quantify the diameter of the partially crystallized structures at the topside of exposure. The crystallization depth was quantified by means of cross sections.

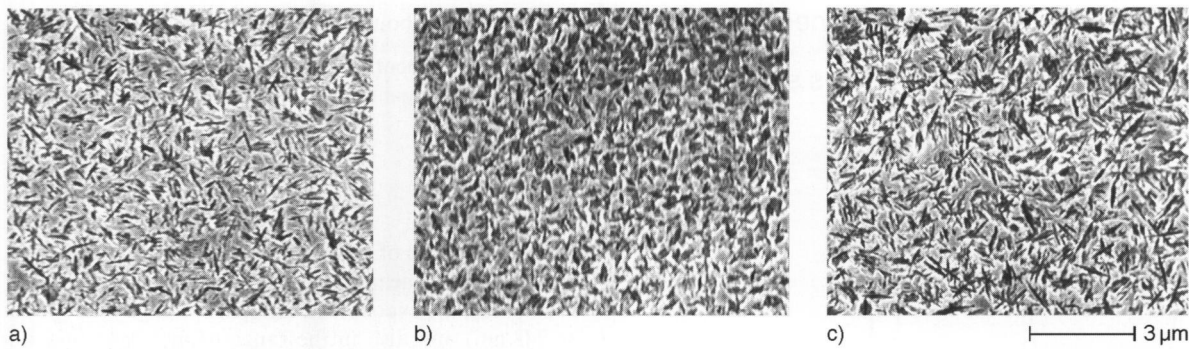
Structural investigation of the crystallized areas took place using a scanning electron microscope (SEM). Previously they were etched in 0.5% hydrofluoric acid for 5 min.

The wet chemical etching process for structuring trenches took place in hydrofluoric acid (10%) at the temperature  $\vartheta = 30$  °C in an ultrasonic bath for 15 min at the most.

## 3. Results and discussion

### 3.1 Crystallization depth

The crystallization depth depends on the optical penetration  $\delta_L$  of UV laser radiation in the glass FS21.  $\delta_L$  is  $> 1000$  μm



Figures 5a to c. SEM pictures after exposure with  $\varepsilon_L = 5 \text{ J/cm}^2$  for different  $\lambda_L$  and constant thermal treatment; a)  $\lambda_L = 248 \text{ nm}$ , b)  $\lambda_L = 308 \text{ nm}$ , c)  $\lambda_L = 355 \text{ nm}$ .

for laser radiation with  $\lambda_L \geq 308 \text{ nm}$ . This has the consequence that all substrates exposed to laser radiation in such a wavelength range were crystallized in the total thickness. For laser exposure with a wavelength in the range of high absorption, the crystallization depth was analyzed for single pulse exposure dependent on  $\varepsilon_L$ . The results for exposure with  $\lambda_L = 248 \text{ nm}$  are shown in figure 3.

The highest crystallization depth  $h_C = (338 \pm 10) \mu\text{m}$  was found for the single pulse exposure.

### 3.2 Geometry of crystallized areas at the top side of exposure

There are differences in lateral geometry of structures after thermal treatment between the exposure to excimer laser radiation and  $(3\omega)\text{Nd:YAG}$  solid state laser radiation. Figures 4a and b show crystallized structures exposed with  $\lambda_L = 248 \text{ nm}$  (figure 4a) and with  $\lambda_L = 355 \text{ nm}$  (figure 4b).

Excimer laser radiation has a so-called top hat beam profile. A part of the laser beam was decoupled and imaged over an optical system on the substrate surface by means of a hole aperture. The steep slope of the edge leads to a nearly homogeneous intensity distribution of the local beam profile. Therefore, the widths of crystallized structures are in the range of the diameter of the laser beam at the image surface. In contrast to this the widths of crystallized structures after exposure to the solid state laser radiation were always smaller than the diameter of the laser beam at the image surface. In addition it was found that the contrast between unlighted glass and crystallized areas is inferior compared to the exposure to the excimer laser radiation. The reason is the slight slope of the edge of the Gaussian laser beam profile of the  $(3\omega)\text{Nd:YAG}$  laser. It was also found that the widths of crystallized structures increased with increasing energy density at exposure. The reason for this is the local overtravel of threshold energy densities necessary in the beam profile of one pulse for the photochemical reaction.

### 3.3 Structural investigation of crystallized areas

For some samples the size of the lithium metasilicate crystals was quantified by means of SEM analysis. The crystals are orderless and interlocked in the structure. So it is quite

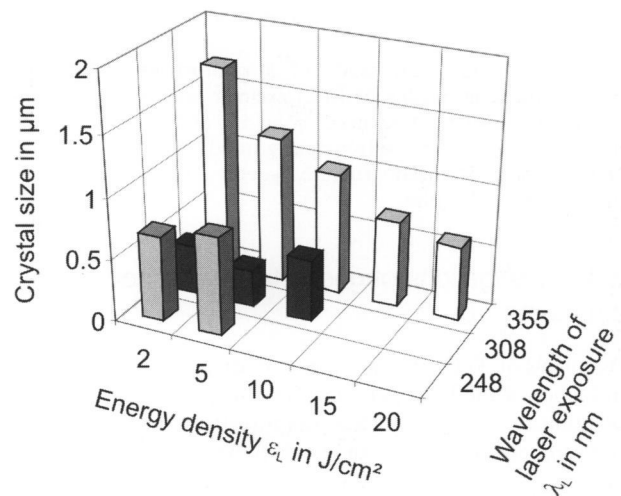


Figure 6. Size of lithium metasilicate crystals  $d_{EK}$  in the texture depending on  $\lambda_L$  and  $\varepsilon_L$  after constant thermal treatment.

difficult to examine the size of single crystals. Structures of crystallized areas after exposure with different  $\lambda_L$  but constant thermal treatment are shown in figures 5a to c. Figure 6 shows the crystal size depending on  $\lambda_L$  and  $\varepsilon_L$ . A dependence of the crystal size on  $\varepsilon_L$  was found only for the exposure with  $\lambda_L = 355 \text{ nm}$ . The crystal size decreases with an increasing of  $\varepsilon_L$ .

The structure of the crystallized areas will be specified by number and size of crystals. It is clear that the finest structure is possible if many and small crystals are grown during the thermal treatment. The finest structure was found for exposure to XeCl excimer laser radiation ( $\lambda_L = 308 \text{ nm}$ ). In this case the crystals are obviously smaller (size  $\approx 300 \text{ nm}$ ) than after exposure with  $\lambda_L = 248 \text{ nm}$  and  $\lambda_L = 355 \text{ nm}$ .

A fine structure of crystallized areas is important for the geometrical microstructuring process. It has a positive effect on the geometrical resolution of microstructures, the surface roughness in microstructures and not least on the etch ratio between unlighted glass and partially crystallized areas.

Furthermore, the dependence of the crystal size on  $\varepsilon_L$ , detected for exposure with  $\lambda_L = 355 \text{ nm}$ , offers the possibility of tuning the crystals to specific sizes for instance for different surface roughness in geometrical microstructures.

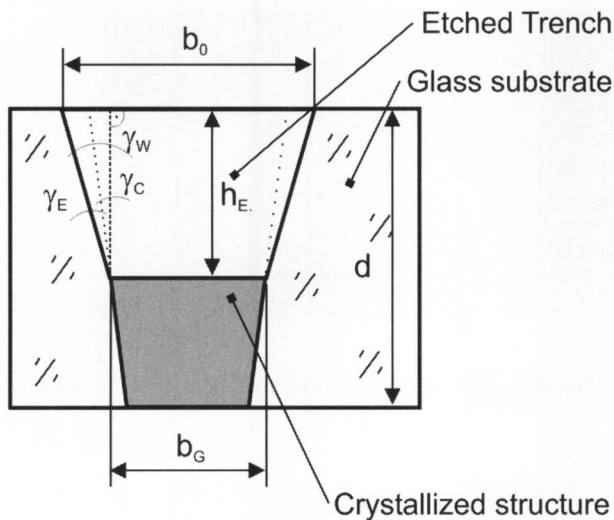


Figure 7. Geometrical ratios of a photostructured trench, manufactured by means of XeCl excimer laser radiation; notations:  $d$ : substrate thickness,  $b_0$ : width of the trench at the topside,  $b_G$ : width of the trench at ground,  $h_E$ : etch depth,  $\gamma_C$ : angle of the crystallized structure,  $\gamma_E$ : etch angle,  $\gamma_w$ : wall angle of the etched structure.

### 3.4 Investigations of geometrically defined microstructures

By means of XeCl excimer laser radiation ( $\lambda_L = 308$  nm) the influence of the laser parameters  $\epsilon_L$  and  $N$  on the geometry of photostructured trenches was investigated. A scheme of the geometrical ratios is shown in figure 7.

Differences between the width of crystallized structures on the topside and on the underside of exposure result in an angle of the crystallized structure  $\gamma_C$ . The wall angle of the trenches  $\gamma_w$  is the sum of an angle of the crystallized structure  $\gamma_C$  and an etch angle  $\gamma_E$ , caused by the etch rate ratio between unexposed glass and crystallized area. It is possible to form the angle of the crystallized structure by means of changing the local focus position, beam shaping and beam delivery. Here is a high potential for various indentation free structures for further investigations. More de-

tailed information about the structuring is published in [4].

In these experiments an etch angle  $\gamma_E = (5 \pm 1)^\circ$  was determined. That means an etch rate ratio of 1:10.

## 4. Summary

Besides the exposure of the photostructurable glass FS21 to UV laser radiation near the absorption maximum of  $Ce^{3+}$  ( $\lambda_L = 308$  nm), the exposure in the range of high absorption ( $\lambda_L = 248$  nm) and also in the range of high transmission ( $\lambda_L = 355$  nm) of the glass is possible. The crystallization depth  $h_C$  depends on the optical density  $\delta_L$ . A crystallization depth at the most of  $h_C = (338 \pm 10)$   $\mu\text{m}$  for an exposure with  $\lambda_L = 248$  nm was found. For exposure to XeCl excimer laser radiation ( $\lambda_L = 308$  nm) the smallest lithium metasilicate crystals were found with a size of  $\approx 300$  nm. Photostructured trenches were manufactured by using XeCl excimer laser radiation ( $\lambda_L = 308$  nm). Therefore, an etch rate ratio of 1:10 between unlighted glass and crystallized area was found.

\*

The authors thank the RWTH Aachen, chair of laser technology, for the realization of the UV-laser exposure experiments.

## 5. References

- [1] Hülsenberg, D.: Glasses for microsystems technology. *Microelectron. J.* **28** (1997) pp. 419–432.
- [2] Harnisch, A.: Beitrag zur Entwicklung von Herstellungstechnologien für komplexe Bauteile aus mikrostrukturierem Glas. Technische Universität Ilmenau, dissertation 1998.
- [3] Stookey, S. D.: Photosensitive glass. *Ind. Eng. Chem.* **41** (1949) no. 4, pp. 856–861.
- [4] Brokmann, U.; Harnisch, A.; Hülsenberg, D.: Einfluss von UV-Laserparametern auf die geometrische Strukturierung von fotosensitivem Glas. *Materialwiss. Werkstofftech.* **34** (2003) no. 7, pp. 666–670.

■ E504P006

Contact:

Ulrike Brokmann  
Technische Universität Ilmenau  
Pf 10 05 65  
D-98684 Ilmenau  
E-mail: Ulrike.Brokmann@Tu-Ilmenau.de